Direct measurement of triaxial strain fields around ferroelectric domains using X-ray microdiffraction

ROBERT C. ROGAN[1], NOBUMICHI TAMURA[2], GEOFFREY A. SWIFT[1] AND ERSAN ÜSTÜNDAG*[1]

[1]Department of Materials Science, California Institute of Technology, Keck Laboratory, Pasadena, California 91125, USA

[2]Advanced Light Source, Lawrence Berkeley National Laboratory, Berkeley, California 94720, USA

*e-mail: ersan@caltech.edu

Published online: 18 May 2003; doi:10.1038/nmat901

Ferroelectric materials, such as $BaTiO_3$, have piezoelectric properties that make them attractive for microelectronic and sensing applications[1]. It is well known that the application of mechanical stress or electric field can alter the domain structure in ferroelectrics[1–6]. Indeed, the constitutive behaviour of a ferroelectric is largely governed by the formation, movement and interaction of its domains. Therefore, it is crucial that the micromechanics of domains and their effect on internal stresses in ferroelectrics be understood. Here we show that the emerging technique of scanning X-ray microdiffraction[7] can be used to measure directly, for the first time, the local triaxial strain fields around 90° domains in single-crystal $BaTiO_3$. Specifically, residual strain maps in a region surrounding an isolated, approximately 40 μm wide, 90° domain were obtained with 3 μm resolution, revealing significant residual strains. This information is critical for accurate micromechanical modelling of domain behaviour in ferroelectrics.

$BaTiO_3$ undergoes a cubic-to-tetragonal phase transition below the Curie temperature (120 °C), which can induce residual stresses, especially in regions under constraint. Because $BaTiO_3$ is also ferroelectric below 120 °C, it is affected by electrical fields leading to a complicated internal stress state[1]. To relieve these stresses, two types of twin structures ('domains') often form in $BaTiO_3$: 90° domains attempt to relieve mechanical stress, whereas 180° domains try to minimize electrostatic energy[8].

Studies have shown that large strains (up to 0.8%) can be induced in $BaTiO_3$ single crystals by activating 90° domain switching (when the *c* axis is reoriented by 90°)[1,4]. Additionally, crystals with engineered domain configurations exhibit high piezoelectric responses[6]. For these reasons, $BaTiO_3$ ceramics are a good candidate for sensor and actuator applications. However, $BaTiO_3$ is susceptible to fatigue and cracking under cyclic electromechanical loading, which currently limits its incorporation into such devices[1,4]. Therefore, the successful application of $BaTiO_3$ requires a detailed understanding of the micromechanics of its domains, and how they influence its damage evolution.

Ferroelectric domains have been observed using various techniques including transmission electron microscopy (TEM)[9], optical microscopy[10] and atomic force microscopy (AFM)[5,8,9,11]. Models of 90° domain boundaries based on X-ray diffraction and high-resolution TEM (HRTEM) have been proposed[12]. TEM and HRTEM methods are hindered by the necessity for extremely thin sample dimensions, and offer limited quantification of strain. Although AFM studies have been successful in outlining the extent of polarization variations across domain boundaries, they offer no information on the value and distribution of lattice strain. Studies using optical birefringence[13,14] have been more promising in this regard, because they yielded some local strain data around domains. Although they offer good spatial resolution, birefringence experiments are only applicable to transparent specimens, and rely on a set of assumptions to obtain a strain value indirectly. Moreover, they cannot distinguish tensile from compressive strain. X-ray diffraction avoids these pitfalls and yields a direct measure of strain by tracking changes in the lattice constants of a crystal. Synchrotron X-ray diffraction has been used to image domains

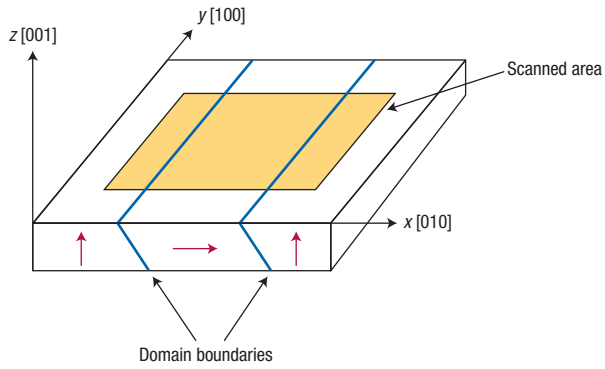

Figure 1 The sample geometry (not to scale). The width of the *a* domain was about 40 μm. The sample measured 5 × 5 × 1 mm³. The scan area was 150 μm (along *x*) by 200 μm (along *y*). The arrows on the side surface indicate the polarization vectors in each domain.

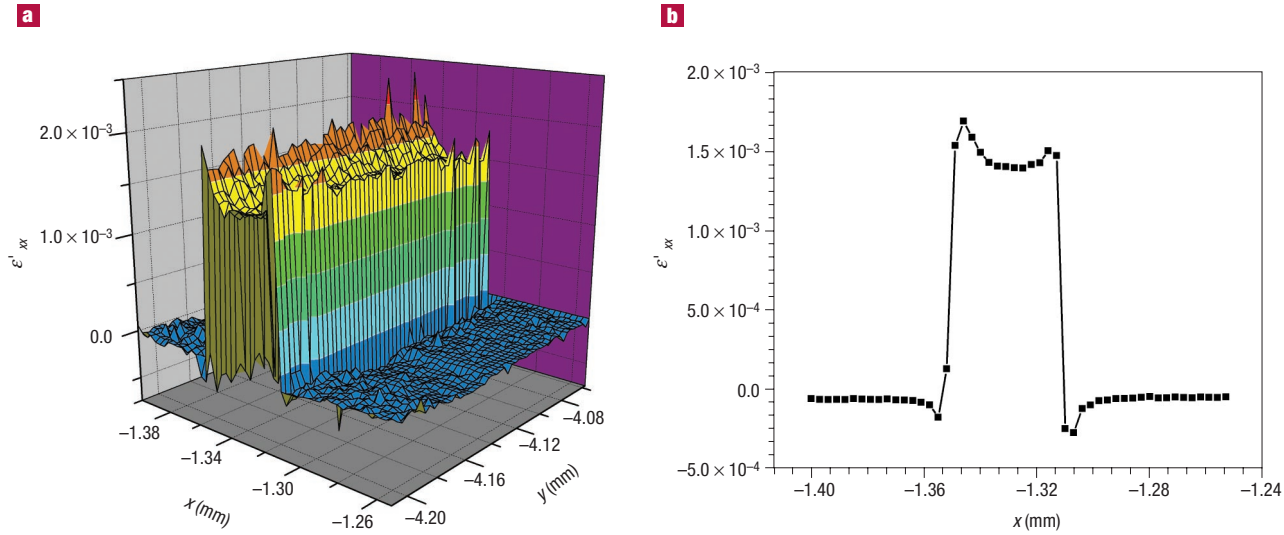

Figure 2 Variation of ε'_{xx} around a single, 90° domain in $BaTiO_3$. a, Two-dimensional variation; **b**, *y*-integrated average. The least-squares fitting routine estimated a typical strain error of about 10^{-5} for all strain data.

by topography[15] and phase contrast[16]. However, no direct measurement of the strain field around a ferroelectric domain has been performed before the present study.

As a first step in an extensive investigation of the micromechanics of ferroelectric domains, this letter presents results on local, triaxial strain fields around 90° domain boundaries. Scanning X-ray microdiffraction (μSXRD) with a polychromatic beam was used to yield strain and crystal orientation data in $BaTiO_3$. μSXRD uses X-rays at medium energies (5–14 keV), collecting data from depths approaching 100 μm in most practical materials. Such penetration depths are several orders of magnitude larger than those achievable by electron microscopy and yield data less influenced by surface effects.

The present study used a single crystal of $BaTiO_3$ obtained from the MTI Corporation (Richmond, California 94804, USA). The sample measured 5 × 5 × 1 mm^3, and was grown in the [001] orientation (normal parallel with the short sample dimension). Its purity was 99.99%, and had a density of 6.02 g cm^{-3}. Both of its (001) faces were polished to a final roughness of less than 15 Å. The presence of 90° domains was confirmed with polarized light microscopy before μSXRD studies.

The μSXRD experiment was conducted at end-station 7.3.3 of the Advanced Light Source, Lawrence Berkeley National Laboratory. After initial alignment, the beam cross-section was measured to be around 1 × 1 μm^2 by scanning a sharp object (a 'knife edge' or a thin wire) under the X-ray beam and collecting the transmitted (or alternatively the fluorescence) signal. The X-ray energy assured that 99% of the diffracted X-rays originated from an approximately 70-μm-deep layer beneath the sample surface[17]. The sample was mounted on a translation stage with its (001) face at an angle of ~45° with respect to the horizontal incident beam. At each position, the crystal was exposed to X-rays for 1 second. The reflection Laue patterns produced by the polychromatic radiation were recorded using a CCD detector (Bruker 6000, with an active area of 90 × 90 mm^2). The data were analysed with a special indexing software using non-linear least-squares refinement[7,18]. Geometrical calibration parameters (sample-to-detector distance, CCD centre positions, detector pitch and yaw) were determined by using a section of the $BaTiO_3$ crystal far from any domain boundary, a region that also served as a reference for strain calculations. In this procedure, the literature values of the $BaTiO_3$ lattice constants at room temperature were used[19]: a = 3.9947 Å and c = 4.0336 Å. As a result, crystal orientation and the triaxial deviatoric strain tensor were obtained for every scanned location.

Figure 1 shows the laboratory coordinate system and its orientation with respect to the crystal axes. Here, z is the normal direction to the sample surface and x and y are in-plane orthogonal directions. An isolated, approximately 40-μm-wide 90° domain was identified in the crystal with its c axis parallel to sample surface (an 'a' domain). It was surrounded by a 'matrix' region where the c axis was perpendicular to sample surface (a 'c' domain). A two-dimensional scan of the area around this isolated domain was performed (Fig. 1). Step sizes in both the x and y directions were 3 μm and the total scanned area measured 150 × 200 μm^2. The indexation of the Laue patterns showed that the c domain had a crystal orientation of (within 0.1°) $[010]\|x$, $[100]\|y$ and $[001]\|z$, while the a domain had the approximate orientation of $[001]\|x$, $[100]\|y$ and $[010]\|z$. (The reader should note the usual 180° ambiguity in diffraction data when interpreting these results.) Another area scan over the side (x–z) surface of the crystal confirmed these orientation relationships. The exact value of the angular separation between the c axes in both domains was 88.5°, which compares well to the theoretical value $(2\tan^{-1}(a/c) = 89.4°$, calculated using the lattice constants given above).

Figure 2a is a three-dimensional representation of the local distribution of the deviatoric component of the residual strain tensor along the x axis (ε'_{xx}) obtained from the two-dimensional scan of the top surface. The maximum observed residual strain (ε'_{xx}) at the domain boundary exceeded 0.15%. This strain was still substantial inside the a domain, and reached different values across each domain boundary. It exhibited minimal variation parallel to the domain boundaries on the sample surface (that is, along the y axis). The asymmetry of the y-integrated profile (Fig. 2b) was also observed in line scans of other domains in this and other samples (data not shown). However, this asymmetry was not always present, nor was it always in the same direction across domain boundaries. Its physical cause is undocumented in previous literature and currently unknown to the authors. The often observed surface relief that accompanies 90° domains[5,20] may have an influence on this strain asymmetry. The fact that XRD effectively

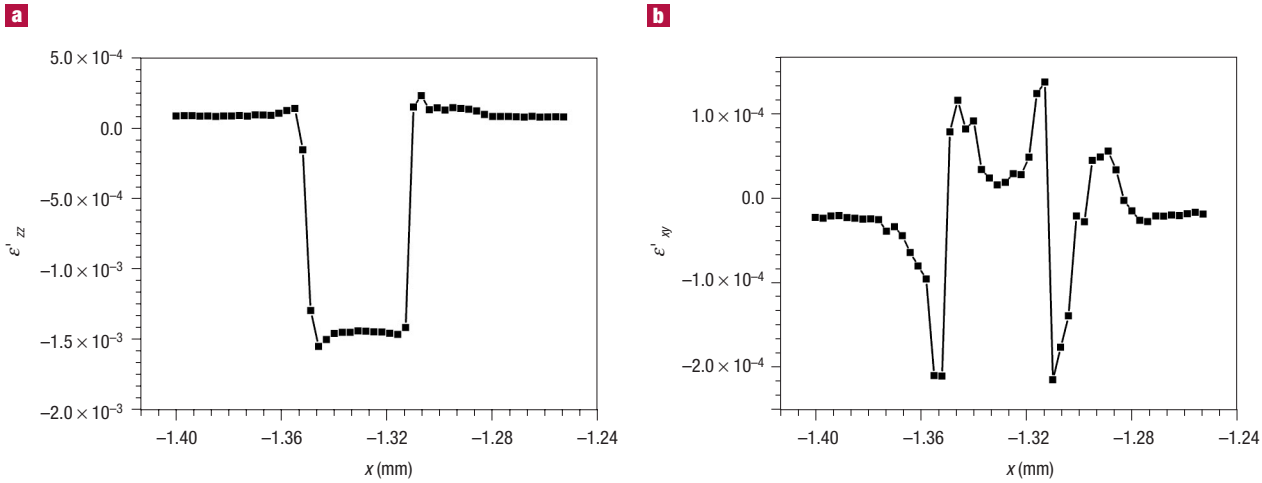

Figure 3 ***y*-integrated average of two strain components in the same region as in Fig. 2. a**, ε'_{zz} (along surface normal); **b**, ε'_{xy} (in-plane shear). Note that the strain axis in (**b**) is different to that in (**a**).

integrates data through depth may be another factor. A systematic investigation of different domain strain states is currently underway. The only other strain-tensor components that displayed significant values for this domain were the shear component ε'_{xy} and the normal component ε'_{zz}. Their *y*-integrated strain profiles along the *x* axis are displayed in Fig. 3a and b, respectively. It is seen that strain along *z* is negative corresponding to compression, whereas the shear strain is positive inside the *a* domain and negative around the domain boundaries. The asymmetry along the *x* direction is noted here, too.

Such spatially resolved strain information is critical for developing realistic micromechanical models of domain wall formation, motion and switching[21]. Preliminary modelling of a similar domain structure using the energy minimization method largely confirmed the observed strain state (positive ε'_{xx} and negative ε'_{zz}). However, the origin of the strain asymmetry is still unknown. Current work at Caltech includes integrated modelling and experimentation, the latter comprising a study of domain structure, kinetics and strain fields under applied electromechanical loading.

In conclusion, polychromatic μSXRD provided direct measurements of lattice distortions in the vicinity of 90° domain boundaries in $BaTiO_3$ for the first time. Residual strain fields were observed to extend several micrometres from domain walls, in contrast to both theoretical calculations and TEM measurements, which indicate that the total domain wall width would not exceed 100 Å[12]. A previously un-noted asymmetry as a function of position was observed in some components of the deviatoric strain tensor. In the future, it is envisaged that comprehensive μSXRD studies of multiple domains will probe the nature and preponderance of the observed asymmetries, and offer insight into the regulating mechanisms of domain equilibrium near surfaces. It is expected that a detailed description of the constitutive behaviour of ferroelectrics, based on domain micromechanics, will emerge from this work.

Received 27 February 2003; accepted 17 April 2003; published 18 May 2003.

References

1. Jaffe, B., Cook, W. R. & Jaffe, H. *Piezoelectric Ceramics* 53–114 (Academic, London, 1971).
2. Li, X. P. *et al.* Effect of a transverse tensile stress on the electric-field- induced domain reorientation in soft PZT: In situ XRD study. *J. Am. Ceram. Soc.* **85,** 844–850 (2002).
3. Kim, S., Gopalan, V. & Gruverman, A. Coercive fields in ferroelectrics: A case study in lithium niobate and lithium tantalate. *Appl. Phys. Lett.* **80,** 2740–2742 (2002).
4. Burcsu, E., Ravichandran, G. & Bhattacharya, K. Large strain electrostrictive actuation in barium titanate. *Appl. Phys. Lett.* **77,** 1698–1700 (2000).
5. Munoz-Saldana, J., Schneider, G. A. & Eng, L. M. Stress induced movement of ferroelastic domain walls in $BaTiO_3$ single crystals evaluated by scanning force microscopy. *Surf. Sci.* **480,** L402–L410 (2001).
6. Wada, S. *et al.* Enhanced piezoelectric property of barium titanate single crystals with engineered domain configurations. *Jpn J. Appl. Phys. Part 1* **38,** 5505–5511 (1999).
7. Tamura, N. *et al.* Submicron x-ray diffraction and its applications to problems in materials and environmental science. *Rev. Sci. Instrum.* **73,** 1369–1372 (2002).
8. Arlt, G. Twinning in ferroelectric and ferroelastic ceramics - stress relief. *J. Mater. Sci.* **25,** 2655–2666 (1990).
9. Arlt, G., Hennings, D. & Dewith, G. Dielectric properties of fine-grained barium-titanate ceramics. *J. Appl. Phys.* **58,** 1619–1625 (1985).
10. Merz, W. J. Domain formation and domain wall motions in ferroelectric $BaTiO_3$ single crystals. *Phys. Rev.* **95,** 690–698 (1954).
11. Hamazaki, S. I., Shimizu, F., Kojima, S. & Takashige, M. AFM observation of 90-Degrees domains of $BaTiO_3$ butterfly crystals. *J. Phys. Soc. Jpn* **64,** 3660–3663 (1995).
12. Floquet, N. *et al.* Ferroelectric domain walls in $BaTiO_3$: Fingerprints in XRPD diagrams and quantitative HRTEM image analysis. *J. Phys. III* **7,** 1105–1128 (1997).
13. Yang, T. J. & Mohideen, U. Nanoscale measurement of ferroelectric domain wall strain and energy by near-field scanning optical microscopy. *Phys. Lett. A* **250,** 205–210 (1998).
14. Yang, T. J., Gopalan, V., Swart, P. J. & Mohideen, U. Direct observation of pinning and bowing of a single ferroelectric domain wall. *Phys. Rev. Lett.* **82,** 4106–4109 (1999).
15. Kim, S., Gopalan, V. & Steiner, B. Direct x-ray synchrotron imaging of strains at 180 degree domain walls in congruent $LiNbO_3$ and $LiTaO_3$ crystals. *Appl. Phys. Lett.* **77,** 2051–2053 (2000).
16. Hu, Z. W. *et al.* Phase-mapping of periodically domain-inverted $LiNbO_3$ with coherent X-rays. *Nature* **395,** 306–306 (1998).
17. Noyan, I. C. & Cohen, J. B. *Residual Stress: Measurement by Diffraction and Interpretation* 110 (Springer, New York, 1987).
18. Tamura, N. *et al.* Scanning X-ray microdiffraction with submicrometer white beam: a new tool for strain/stress and orientation mapping in thin films. *J. Synchrotron Radiat.* **10,** 137–143 (2003).
19. Wyckoff, R. W. G. *Crystal Structures* (Wiley, New York, 1964).
20. Ganpule, C. S. *et al.* Imaging three-dimensional polarization in epitaxial polydomain ferroelectric thin films. *J. Appl. Phys.* **91,** 1477–1481 (2002).
21. Shu, Y. C. & Bhattacharya, K. Domain patterns and macroscopic behaviour of ferroelectric materials. *Philos. Mag. B* **81,** 2021–2054 (2001).

Acknowledgements

R. C. Rogan is supported by the Multidisciplinary University Research Initiative at Caltech on Engineering Microstructural Complexity in Ferroelectric Devices (Army Research Office grant no. DAAD19-01-1-0517). E. Üstündag is partially funded by the National Science Foundation (CAREER grant no. DMR-9985264). The Advanced Light Source is supported by Office of Basic Energy Sciences, the US Department of Energy under contract no. DE-AC03-76SF00098. The $BaTiO_3$ specimen was provided by G. Ravichandran from the Caltech Corporation. Insightful discussions with K. Bhattacharya and W. Zhang are gratefully acknowledged.
Correspondence and requests for materials should be addressed to E.Ü.

Competing financial interests

The authors declare that they have no competing financial interests.